

Original article

Chronic Interstitial Pneumonia in Young Patients Undergoing Lung Transplantation or Autopsy: Clinico-radiologic-pathologic Observations from a Single Institution

Mayu Uka, MD ¹⁾, Toshihiro Iguchi, MD ¹⁾, Katsuya Kato, MD ²⁾, Hidehiro Hayashi, MD ³⁾,
Ichiro Yamadori, MD ⁴⁾, Toshiharu Mitsuhashi, MD ⁵⁾, Takahiro Oto, MD ⁶⁾, Shuhei Sato, MD ¹⁾,
Susumu Kanazawa, MD ¹⁾

Departments of Radiology ¹⁾ and General Thoracic Surgery ⁶⁾, and Center for Innovative Clinical
Medicine ⁵⁾, Okayama University Medical School, 2-5-1 Shikata-cho, kita-ku Okayama
700-8558, Japan

Department of Diagnostic Radiology ²⁾, Kawasaki Hospital, Kawasaki Medical School

Department of Radiology ³⁾, Okayama Red Cross Hospital

Department of Pathology ⁴⁾, Hiroshima City Hiroshima Citizens Hospital

Correspondence to: Toshihiro Iguchi

Department of Radiology, Okayama University Medical School, 2-5-1 Shikata-cho, kita-ku

Okayama 700-8558, Japan

E-mail: iguchi@ba2.so-net.ne.jp

Phone: +81-86-235-7313, Fax: +81-86-235-7316

The authors declare no conflicts of interest or funding sources to disclose.

Abstract

Purpose

To retrospectively evaluate high-resolution computed tomography (HRCT) findings and clinical diagnoses of chronic interstitial pneumonia (IP) with a poor prognosis in young patients (≤ 50 years).

Materials and methods

HRCT images of 8 men and 7 women (mean age, 34.8 years) obtained before lung transplantation or autopsy were reviewed. After reviewing whole lung specimens and pathologic diagnoses, all patients were clinically diagnosed according to the 2010 idiopathic pulmonary fibrosis/usual interstitial pneumonia (IPF/UIP) consensus statement.

Results

HRCT images revealed intralobular reticular opacity, air cysts, ground glass opacity, traction bronchiectasis, and interlobular septal thickening. Intralobular reticular opacity was the most extensive finding. Abnormal findings existed predominantly in both the peripheral and lower lung zones in only 1 patient. Classifications of HRCT patterns were “UIP” (n = 2), “inconsistent with UIP” (n = 11), and “indeterminate UIP” (n = 2). Multidisciplinary diagnoses were “IPF/UIP” (n = 1), “possible IPF/UIP” (n = 1), “IP with connective tissue disease” (n = 7), “fibrotic nonspecific IP” (n = 1), and “unclassified IP” (n = 5).

Conclusion

The most extensive HRCT finding was intralobular reticular opacity. Most HRCT

1 images differed from typical IPF/UIP, and IPF/UIP was uncommon in young patients with
2
3
4 chronic IP with a poor prognosis.
5
6
7
8

9 **Keywords**

10
11
12 Chronic interstitial pneumonia, Young, High-resolution computed tomography
13
14
15
16
17
18
19
20
21
22
23
24
25
26
27
28
29
30
31
32
33
34
35
36
37
38
39
40
41
42
43
44
45
46
47
48
49
50
51
52
53
54
55
56
57
58
59
60
61
62
63
64
65

Introduction

Chronic interstitial pneumonia (IP) with a poor prognosis is uncontrollable and intractable. Usually, this disease occurs in the elderly (> 50 years), and the majority are clinically diagnosed with idiopathic pulmonary fibrosis (IPF)/usual interstitial pneumonia (UIP). There is no proven pharmacological therapy for IPF/UIP [1] and its prognosis was reported as having a median survival of < 3 years [2, 3]. Conversely, in the young (≤ 50 years), chronic IP with a poor prognosis is not well known.

Nadrous et al. [4] reported that there was no significant difference in clinical, radiological, or pathological features between IPF/UIP in the young versus the elderly; high-resolution computed tomography (HRCT) imaging revealed typical findings of IPF/UIP in 16 of 21 patients < 50 years with IPF/UIP. However, in a clinical situation, HRCT imaging sometimes reveals atypical findings such as IPF/UIP in the young with chronic IP with a poor prognosis. This may be because IPF/UIP is uncommon in the young, unlike in the elderly. An age > 50 years had been 1 minor criterion for a presumptive diagnosis of IPF/UIP based on the 2000 American Thoracic Society (ATS)-European Respiratory Society (ERS) consensus statement [5], although this minor criterion is now removed. However, there have been few large studies of HRCT findings, HRCT diagnosis, and clinical diagnosis of chronic IP with a poor prognosis in the young. In this study, we retrospectively evaluated HRCT findings and clinical diagnoses of chronic IP with a poor prognosis in the young ≤ 50 years.

Materials and methods

Informed consent was obtained from all patients before performing computed tomography (CT). The ethics committee at our institution approved the present retrospective

1 study and waived the requirement for informed consent for the use of medical patient data.

2 3 4 **Patients**

5
6
7 Between October 1998 and December 2010, 115 patients with severe lung disease
8
9 were enrolled in the Japan Organ Transplant Network at our institution. Of these, 17 patients
10
11 with IP fulfilled all of the following criteria of this study: ≤ 50 years, a treatment period ≥ 1 year,
12
13 underwent HRCT, and underwent pathologic diagnosis of the whole lung. Two patients were
14
15 excluded because of unavailable HRCT imaging or iatrogenic IP caused by bone marrow
16
17 transplantation. Thus, 15 patients (8 men and 7 women; mean age, 34.8 years \pm 10.8 [standard
18
19 deviation]; range, 13–50 years) were included in this study (**Table 1**). Thirteen patients
20
21 underwent bilateral lung transplantation and 1 underwent single lung transplantation; 1 died of
22
23 progression of lung disease and underwent autopsy. Four patients had a history of connective
24
25 tissue disease (CTD), 2 had a familial history of IPF/UIP, and 3 had both. Eight patients did not
26
27 meet the criteria of lung-dominant CTD [6], and these 8 patients had neither the clinical nor
28
29 serologic features indicative of IP with autoimmune features, based on the classification criteria
30
31 [7]. No significant occupational exposure was reported in any patient. Four patients had a
32
33 smoking history (mean, 30.6 pack-years; range, 13–62.5 pack-years) and the others had never
34
35 smoked. All patients were resistant to medical therapy and exhibited respiratory depression.
36
37 They fulfilled 1 of the following conditions: vital capacity or total lung capacity under 60% of
38
39 the predictive value, hypoxemia at rest under 60 Torr, or grade III to V dyspnea according to the
40
41 Hugh-Jones classification [8].
42
43
44
45
46
47
48
49
50
51

52 **Evaluation of HRCT findings**

53
54 All patients underwent CT (Aquilion 16 or Aquilion 64; Toshiba Medical Systems
55
56 Corporation, Otawara, Japan; or Light Speed Scanner; GE Healthcare, Milwaukee WI, USA)
57
58
59
60
61
62
63
64
65

1 within 5 months of undergoing lung transplantation or at autopsy. CT images were obtained at
2 the end of inspiration with patients in the supine position. The HRCT scanning protocol
3
4 consisted of the reconstruction of 1–3-mm collimation sections with a high spatial frequency
5
6 algorithm at 1- or 2-cm intervals. CT images were photographed at window settings appropriate
7
8 for viewing the lung parenchyma (window level, -600 to -700 Hounsfield Units; window width,
9
10 1200–1500 Hounsfield Units).
11
12
13
14
15

16
17 HRCT images were reviewed retrospectively by consensus by 3 thoracic radiologists
18
19 with 8, 22, and 33 years of experience, respectively. Observers were blinded to the clinical and
20
21 histological information. Consensus interpretation was simultaneously arrived at by the 3
22
23 radiologists by discussion. The presence of the following 10 abnormal HRCT findings were
24
25 evaluated: intralobular reticular opacity, air cysts (including emphysematous bulla),
26
27 honeycombing, ground glass opacity (GGO), air space consolidation, traction bronchiectasis,
28
29 interlobular septal thickening, thickening of the bronchovascular bundle, distortion, and
30
31 ill-defined centrilobular nodules. These abnormal HRCT findings were defined based on
32
33 previous definitions [9, 10]. If intralobular reticular opacity overlapped with GGO, intralobular
34
35 reticular opacity was given priority. If GGO appeared without reticular opacity, the abnormal
36
37 finding was evaluated as GGO.
38
39
40
41
42
43
44

45 The lungs were divided into 6 zones (the upper, middle, and lower zones in both lungs).
46
47 The upper zone was defined as the lung above the level of the tracheal carina; the lower zone as
48
49 the lung below the level of the inferior pulmonary vein; and the middle zone as the lung portion
50
51 between the upper and lower zones. The extent of involvement of abnormal HRCT findings was
52
53 evaluated visually and independently in each lung zone. For 5 findings (intralobular reticular
54
55 opacity, air cysts, honeycombing, GGO, and air space consolidation), a score was assigned on
56
57
58
59
60
61
62
63
64
65

1 the basis of the percentage of lung parenchyma that showed evidence of abnormal findings and
2 was estimated to the nearest 5% of parenchymal involvement based on the scoring system
3
4 reported by Sumikawa et al. [11]. The overall percentage of involvement (i.e., median and mean
5
6 scores of the 6 lung zones) was calculated.
7
8
9

10
11
12 After assessing the presence and extent of abnormal findings, observers evaluated the
13 predominant distribution of the findings. Predominance was assessed as being in the “upper lung
14 zone,” “lower lung zone,” or as “diffuse lung involvement.” Upper lung zone predominance
15
16 was considered present when most abnormal findings were above the level of the tracheal
17
18 carina; lower zone predominance was considered present when most abnormal findings were
19
20 below this level; and diffuse lung involvement was considered present when neither was
21
22 predominant. The anatomic distribution was also evaluated and noted to be a “peripheral pattern”
23
24 if there was a predominance of abnormal findings in the outer third of the lung, a
25
26 “peribronchovascular pattern” if there was predilection for the peribronchovascular areas, or a
27
28 “diffuse pattern” if there was no predominance. Observers finally classified the cases as a “UIP
29
30 pattern”, “possible UIP pattern”, or “inconsistent with UIP pattern,” according to the 2010
31
32 ATS-ERS consensus statement [1]. In addition, HRCT findings were diagnosed as
33
34 “indeterminate UIP pattern”, according to the categories reported by Chung et al [12], when the
35
36 findings were not suitable for any of these 3 patterns.
37
38
39
40
41
42
43
44
45
46
47

48 **Pathologic and clinical diagnosis**

49

50 All whole lung specimens were reviewed by a lung pathologist with 34 years of
51
52 experience. All pathologic specimens were fixed with 10% formalin, embedded in paraffin wax,
53
54 and stained with hematoxylin-eosin or elastica-Masson stain for conventional microscopy.
55
56

57 Pathologic images were obtained through a digital microscope camera (DS-Fi1; Nikon; Tokyo,
58
59
60
61
62
63
64
65

1 Japan). All patients were classified into subgroups according to the 2010 ATS-ERS consensus
2 statement [1]. Thereafter, all patients were clinically diagnosed according to the consensus
3 statement [1]. Patients were diagnosed with “unclassified IP” when both the multidisciplinary
4 diagnosis did not satisfy the criteria for a UIP pattern and the histologic patterns were not
5 classified as any other type of IP.
6
7
8
9
10
11
12
13

14 **Statistical analysis**

15
16
17 Friedman’s test and Wilcoxon’s signed-rank test with Bonferroni correction were used
18 to compare the extent of 5 abnormal findings (intra-lobular reticular opacity, air cysts,
19 honeycombing, GGO, and air space consolidation). Thereafter, we compared the most extensive
20 finding with the other 4 findings. *P*-values < 0.05 for Friedman’s test and < 0.0125 for
21 Wilcoxon’s signed-rank test with Bonferroni correction were considered statistically significant.
22 All statistical analyses were performed using SPSS software (version 22.0; IBM, Armonk, NY,
23 USA).
24
25
26
27
28
29
30
31
32
33
34
35
36
37

38 **Results**

39
40 A summary of each patient is shown in **Table 1**.
41
42

43 **HRCT findings and diagnosis**

44
45 The mean total extent of parenchymal abnormalities on HRCT was 85% ± 17.
46
47 Intra-lobular reticular opacity, air cysts, GGO, traction bronchiectasis, and interlobular septal
48 thickening were present in all patients. HRCT findings are shown in **Table 2**. The most
49 extensive finding was intra-lobular reticular opacity (median, 37.5%; mean, 39%; interquartile
50 range, 15–65%). The median extent of air cysts, honeycombing, GGO, and air space
51 consolidation was 10% (mean, 19%; interquartile range, 5–20%), 5% (mean, 10%; interquartile
52
53
54
55
56
57
58
59
60
61
62
63
64
65

1 range, 0–10%), 5% (mean, 9%; interquartile range, 5–10%), and 5% (mean, 7%; interquartile
2 range, 5–10%), respectively (**Table 2**). The median maximum size of honeycombing on the
3 HRCT images of the patients was 2.9 mm (mean, 3.5 mm; interquartile range, 1.7–6.0 mm).
4
5
6
7
8
9 Only 1 patient (patient 13) had honeycombing >10 mm.

10
11
12 In multiple comparisons, there were significant differences ($P = 0.01$) by Friedman’s
13 test. Intralobular reticular opacity was significantly higher than 3 other findings (vs. GGO [$P =$
14 0.003], consolidation [$P = 0.001$], and honeycombing [$P = 0.009$]; Wilcoxon’s signed-rank test
15 with Bonferroni correction).
16
17
18
19
20
21

22 Regarding distributions on HRCT images, lower lung predominance, upper lung
23 predominance, and diffuse lung involvement were present in 6, 3, and 6 patients, respectively
24 (**Table 3**). The anatomic distributions were noted to be a peripheral pattern, peribronchovascular
25 pattern, and diffuse pattern in 3, 5, and 7 patients, respectively (**Table 3**). The diagnoses from
26 HRCT findings were UIP pattern ($n = 2$; **Fig. 1**), inconsistent with UIP pattern ($n = 11$; **Fig. 2**),
27 and **indeterminate UIP pattern** ($n = 2$) (**Table 1**). In 2 patients, HRCT findings were diagnosed
28 as “**indeterminate UIP pattern**” because the images showed uniformly diffuse abnormal findings
29 in the whole lung (**Fig. 3**).
30
31
32
33
34
35
36
37
38
39
40
41

42 **Pathologic and clinical diagnosis**

43
44
45 The pathologic diagnoses were “UIP” ($n = 5$), “probable UIP” ($n = 4$), “possible UIP”
46 ($n = 1$) and “not UIP” ($n = 5$). Microscopic honeycombing was seen in 13 cases (87%).
47

48 However, most honeycombing was very small (<2 mm) and included mucus retention. None of
49 patients, except for those diagnosed as having IP with CTD, had pathological features indicative
50 of IP with autoimmune disease. Intralobular reticular opacities on the HRCT images
51 corresponded to marked fibrosis such as bridging fibrosis in the pathologic findings.
52
53
54
55
56
57
58
59
60

1
2 Multidisciplinary diagnoses were IPF/UIP (n = 1), possible IPF/UIP (n = 1), IP with
3
4 CTD (UIP [n = 2], fibrotic nonspecific interstitial pneumonia [NSIP; n = 2], unclassified [n = 3]),
5
6 fibrotic NSIP (n = 1), and unclassified IP (n = 5).
7

8
9 One patient, whose HRCT diagnosis was “**indeterminate UIP pattern**” and
10
11 pathological diagnosis was “probable UIP”, was diagnosed as having unclassified IP. In 4 of 8
12
13 patients who did not meet the criteria of CTD, pathological findings revealed marked
14
15 centrilobular fibrosis and bridging fibrosis, which are common in chronic hypersensitivity
16
17 pneumonitis (CHP). However, because they had neither the other pathologic features nor
18
19 clinical features of CHP, their pathologic diagnosis was “not UIP” and the multidisciplinary
20
21 diagnosis was “unclassified IP.”
22
23
24
25
26
27
28
29

30 **Discussion**

31
32 Several diseases, such as IPF/UIP, familial IPF, and CTD-related IP were reported as
33
34 chronic IP in the young < 50 years [4]. IPF/UIP was uncommon in our 15 younger patients; only
35
36 2 patients (13%) were clinically diagnosed with IPF/UIP.
37
38
39

40
41 Many investigators have already reported detailed HRCT findings of IPF/UIP [11–16].
42
43 Honeycombing is a core finding of IPF/UIP and is helpful when distinguishing this disease from
44
45 other IPs [11]. Abnormal findings exist predominantly in the peripheral and lower lung zones
46
47 [11, 13, 17]. Additionally, GGO and reticular opacity were reported as other predominant
48
49 findings [17]. The majority of our HRCT findings were different from typical findings of
50
51 IPF/UIP. Our results showed an extremely large disease extent (mean, 85%) in the whole lung
52
53 compared with previous reports (34.1% [11] and 20.17–28.60% [18]). In addition, intralobular
54
55 reticular opacity was the most extensive finding (median and mean scores, 37.5% and 39%,
56
57
58
59
60
61
62
63
64
65

1
2 respectively). Conversely, the honeycombing score (median and mean, 5% and 10%,
3
4 respectively) was not so different in extent in the whole lung, in contrast with previous reports
5
6 (mean score, 4.4% [11] and 7.04% [18]). Furthermore, distributions were different from those of
7
8 typical IPF/UIP: abnormal findings existed predominantly in both the peripheral and lower lung
9
10 zones in only 1 patient (7%).
11
12

13
14 The wider extent of abnormal findings on HRCT images in the present study seemed
15
16 to be consistent with the findings of end-stage IP. Honeycombing was said to enlarge slowly
17
18 over time [14, 19]. However, honeycombing on the HRCT images was smaller in our study than
19
20 in previous reports [19]. Honeycombing was observed pathologically in all patients, except 2
21
22 patients, although most honeycombing was smaller than 2 mm and included mucus retention.
23
24 Therefore, honeycombing could not be detected on HRCT. Although 10 patients were
25
26 pathologically diagnosed with UIP, probable UIP, or possible UIP, only 2 were diagnosed with
27
28 UIP pattern based on HRCT images. We presumed that another reason for the discrepancy
29
30 between the HRCT and pathologic findings was as follows: the craniocaudal distributions were
31
32 different from those of typical IPF/UIP. Upper or mid-lung predominance is 1 HRCT criterion
33
34 for “inconsistent with UIP pattern” [1]; upper lung predominance was seen in 3 patients (20%).
35
36
37
38
39
40
41
42

43 Our results showed that reticular opacity was the most common finding on HRCT
44
45 imaging, although it was unclear whether this finding existed from an early stage because the
46
47 patients’ progress was not followed from an early stage. If reticular opacity exists in the majority
48
49 of patients with early-stage IP with a poor prognosis but does not exist in patients with IP with a
50
51 better prognosis, this finding may be a predictor of poor convalescence in younger patients with
52
53 IP with a poor prognosis.
54
55
56

57
58 Familial IPF is a rare condition defined as the presence of IPF in at least 2 family
59
60

1 members [5] and is a distinct entity that should be considered separately from non-familial IPF
2
3
4 [20]. In our study, 2 patients (13%) had familial IPF without CTD. Familial IPF accounts for
5
6 less than 5% of all patients with IPF [21–23]. Nadrous et al. [4] reported that 3 (14%) of 22
7
8 IPF/UIP patients < 50 years had familial histories. Nishiyama et al. [24] reported that the HRCT
9
10 findings of familial IPF resemble those of sporadic IPF; however, familial IPF had a lower
11
12 prevalence of honeycombing and a lower prevalence of a lower lung predominant distribution
13
14 than non-familial IPF. Among our 2 patients, there was no case with a typical UIP pattern on
15
16 HRCT; their abnormalities showed diffuse patterns and diffuse lung involvement.
17
18
19
20
21

22 Patients with CTD-related UIP were younger than patients with IPF/UIP [18, 25].

23
24 Patients may subsequently manifest overt features of an underlying CTD that was subclinical at
25
26 the time IP was diagnosed [25]. Patients with CTD-related IP have a better prognosis than
27
28 patients with idiopathic IP [26, 27]. However, IP is referred to as 1 factor related to a poor CTD
29
30 prognosis [28]. The present study included 7 patients (47%) with a history of CTD. No patient
31
32 except 1 was diagnosed with UIP pattern based on HRCT findings, while 5 of 7 were diagnosed
33
34 as having UIP/probable UIP based on pathologic findings. This discrepancy may be because
35
36 honeycombing was hidden in reticular shadows on HRCT images. Kono et al. [25] reported that
37
38 HRCT imaging showed no statistically significant difference between the CTD-related UIP and
39
40 IPF/UIP groups with regard to the presence or distribution of each finding. Conversely, Song et
41
42 al. [18] reported that patients with CTD-related IP often had atypical IPF/UIP patterns and had
43
44 marginally significantly lower scores for honeycombing compared with IPF/UIP patients; their
45
46 results were similar to ours.
47
48
49
50
51
52
53
54

55 This retrospective study enrolled a small number of patients, and there was the
56
57 potential for a patient selection bias, as all patients were from a single institution. Only a small
58
59
60
61
62
63
64
65

1 proportion of younger patients with chronic IP with a poor prognosis were evaluated. Three
2 radiologists simultaneously performed a consensus interpretation of evaluation of HRCT
3 findings. The results may have been affected by the senior radiologist's interpretation. It is very
4 difficult to diagnose CHP histologically [29]. Four patients had the pathological findings of
5 centrilobular fibrosis and bridging fibrosis; however, the multidisciplinary diagnosis was
6 unclassified IP. Therefore, patients with CHP may have actually been included. Our study was
7 not designed to compare the clinical, radiological, and pathological features of the young with IP
8 with a poor prognosis with those with a better prognosis. Additionally, only patients whose
9 whole lung was obtained by transplantation or autopsy were enrolled. Thus, our study
10 enrollment decreased. However, this study is interesting and important because there was no
11 previous report evaluating radiological, pathological, and clinical diagnoses using the whole
12 lung in the young with chronic IP with a poor prognosis. The specimen obtained by surgical
13 biopsy was an evaluation of only a part of the organ, and the condition of the lung at autopsy is
14 worse because of post mortem changes.

15
16
17
18
19
20
21
22
23
24
25
26
27
28
29
30
31
32
33
34
35
36
37
38 In conclusion, the most extensive HRCT finding was intralobular reticular opacity.
39
40 Most HRCT images differed from typical IPF/UIP. IPF/UIP was uncommon in the young with
41 chronic IP with a poor prognosis.
42
43
44
45
46
47
48
49
50
51
52
53
54
55
56
57
58
59
60
61
62
63
64
65

1
2 **References**
3

- 4 1. Raghu G, Collard HR, Egan JJ, Martinez FJ, Behr J, Brown KK, et al. An official
5
6
7
8
9
10
11
12
13
14
15
16
17
18
19
20
21
22
23
24
25
26
27
28
29
30
31
32
33
34
35
36
37
38
39
40
41
42
43
44
45
46
47
48
49
50
51
52
53
54
55
56
57
58
59
60
61
62
63
64
65
1. Raghu G, Collard HR, Egan JJ, Martinez FJ, Behr J, Brown KK, et al. An official
ATS/ERS/JRS/ALAT statement: idiopathic pulmonary fibrosis: evidence-based guidelines for
diagnosis and management. *Am J Respir Crit Care Med.* 2011;183:788–824.
2. King TE Jr, Tooze JA, Schwarz MI, Brown KR, Cherniack RM. Predicting survival in
idiopathic pulmonary fibrosis: scoring system and survival model. *Am J Respir Crit Care Med.*
2001;164:1171–81.
3. Nicholson AG, Colby TV, du Bois RM, Hansell DM, Wells AU. The prognostic significance
of the histologic pattern of interstitial pneumonia in patients presenting with the clinical entity of
cryptogenic fibrosing alveolitis. *Am J Respir Crit Care Med.* 2000;162:2213–7.
4. Nadrous HF, Myers JL, Decker PA, Ryu JH. Idiopathic pulmonary fibrosis in patients
younger than 50 years. *Mayo Clin Proc.* 2005;80:37–40.
5. American Thoracic Society. Idiopathic pulmonary fibrosis: diagnosis and treatment:
international consensus statement. American Thoracic Society (ATS), and European
Respiratory Society (ERS). *Am J Respir Crit Care Med.* 2000;161:646–64.
6. Omote N, Taniguchi H, Kondoh Y, Watanabe N, Sakamoto K, Kimura T, et al.
Lung-dominant connective tissue disease: clinical, radiologic, and histologic features. *Chest.*
2015;148:1438–46.
7. Fischer A, Antoniou KM, Brown KK, Cadranel J, Corte TJ, du Bois RM, et al. An official
European Respiratory Society/American Thoracic Society research statement: interstitial
pneumonia with autoimmune features. *Eur Respir J.* 2015;46:976–87.
8. Hugh-Jones P, Lambert AV. A simple standard exercise test and its use for measuring
exertion dyspnea. *Br Med J.* 1952;1:65–71.

- 1
2 9. Webb WR, Müller NL, Naidich DP. Illustrated glossary of high-resolution CT terms. In:
3
4 High-resolution CT of the lung. 5th ed. Riverwoods, IL: Wolters Kluwer Health; 2015. pp. 660–
5
6 77.
7
8
9 10. Hansell DM, Bankier AA, Macmahon H, McLoud TC, Müller NL, Remy J. Fleischner
10 Society: glossary of terms for thoracic imaging. *Radiology*. 2008;246:697–722.
11
12
13 11. Sumikawa H, Johkoh T, Ichikado K, Taniguchi H, Kondoh Y, Fujimoto K, et al. Usual
14 interstitial pneumonia and chronic idiopathic interstitial pneumonia: analysis of CT appearance
15 in 92 patients. *Radiology*. 2006;241:258–66.
16
17
18 12. Chung JH, Chawla A, Peljto AL, Cool CD, Groshong SD, Talbert JL, et al. CT scan findings
19 of probable usual interstitial pneumonitis have a high predictive value for histologic usual
20 interstitial pneumonitis. *Chest*. 2015;147:450–9.
21
22
23 13. Nishimura K, Kitaichi M, Izumi T, Nagai S, Kanaoka M, Itoh H. Usual interstitial
24 pneumonia: histologic correlation with high-resolution CT. *Radiology*. 1992;182:337–42.
25
26
27 14. Akira M, Sakatani M, Ueda E. Idiopathic pulmonary fibrosis: progression of honeycombing
28 at thin-section CT. *Radiology*. 1993;189:687–91.
29
30
31 15. Hunninghake GW, Lynch DA, Galvin JR, Gross BH, Müller N, Schwartz DA, et al.
32 Radiologic findings are strongly associated with a pathologic diagnosis of usual interstitial
33 pneumonia. *Chest*. 2003;124:1215–23.
34
35
36 16. Lynch DA, Travis WD, Müller NL, Galvin JR, Hansell DM, Grenier PA, et al. Idiopathic
37 interstitial pneumonias: CT features. *Radiology*. 2005;236:10–21.
38
39
40 17. Johkoh T, Müller NL, Cartier Y, Kavanagh PV, Hartman TE, Akira M, et al. Idiopathic
41 interstitial pneumonias: diagnostic accuracy of thin-section CT in 129 patients. *Radiology*.
42 1999;211:555–60.
43
44
45
46
47
48
49
50
51
52
53
54
55
56
57
58
59
60
61
62
63
64
65

- 1
2 18. Song JW, Do KH, Kim MY, Jang SJ, Colby TV, Kim DS. Pathologic and radiologic
3
4 differences between idiopathic and collagen vascular disease-related usual interstitial pneumonia.
5
6 Chest. 2009;136:23–30.
7
8
9 19. Mino M, Noma S, Kobayashi Y, Iwata T. Serial changes of cystic air spaces in fibrosing
10
11 alveolitis: a CT-pathological study. Clin Radiol. 1995; 50:357–63.
12
13
14 20. Katzenstein AL, Myers JL. Idiopathic pulmonary fibrosis. Clinical relevance of pathologic
15
16 classification. Am J Respir Crit Care Med. 1998;157:1301–15.
17
18
19 21. Marshall RP, Puddicombe A, Cookson WO, Laurent GJ. Adult familial cryptogenic
20
21 fibrosing alveolitis in the United Kingdom. Thorax. 2000;55:143–6.
22
23
24 22. Hodgson U, Laitinen T, Tukiainen P. Nationwide prevalence of sporadic and familial
25
26 idiopathic pulmonary fibrosis: evidence of founder effect among multiplex families in Finland.
27
28 Thorax. 2002;57:338–42.
29
30
31 23. Allam JS, Limper AH. Idiopathic pulmonary fibrosis: is it a familial disease? Curr Opin
32
33 Pulm Med. 2006;12:312–7.
34
35
36 24. Nishiyama O, Taniguchi H, Kondoh Y, Kimura T, Katoh T, Oishi T, et al. Familial idiopathic
37
38 pulmonary fibrosis: serial high-resolution computed tomography findings in 9 patients. J
39
40 Comput Assist Tomogr. 2004;28:443–8.
41
42
43 25. Kono M, Nakamura Y, Enomoto N, Hashimoto D, Fujisawa T, Inui N, et al. Usual
44
45 interstitial pneumonia preceding collagen vascular disease: a retrospective case control study of
46
47 patients initially diagnosed with idiopathic pulmonary fibrosis. PLoS One. 2014;9:e94775.
48
49
50 26. Douglas WW, Tazelaar HD, Hartman TE, Hartman RP, Decker PA, Schroeder DR, et al.
51
52 Polymyositis-dermatomyositis-associated interstitial lung disease. Am J Respir Crit Care Med.
53
54 2001;164:1182–5.
55
56
57
58
59
60
61
62
63
64
65

1
2 27. Flaherty KR, Colby TV, Travis WD, Toews GB, Mumford J, Murray S, et al. Fibroblastic
3
4 foci in usual interstitial pneumonia: idiopathic versus collagen vascular disease. Am J Respir
5
6 Crit Care Med. 2003;167:1410–5.
7

8
9 28. Woodhead F, Wells AU, Desai SR. Pulmonary complications of connective tissue diseases.
10
11 Clin Chest Med. 2008;29:149–64.
12

13
14 29. Akashi T, Takemura T, Ando N, Eishi Y, Kitagawa M, Takizawa T, et al. Histopathologic
15
16 analysis of sixteen autopsy cases of chronic hypersensitivity pneumonitis and comparison with
17
18 idiopathic pulmonary fibrosis/usual interstitial pneumonia. Am J Clin Pathol. 2009; 131:405–15.
19
20
21
22
23
24
25
26
27
28
29
30
31
32
33
34
35
36
37
38
39
40
41
42
43
44
45
46
47
48
49
50
51
52
53
54
55
56
57
58
59
60
61
62
63
64
65

1
2 **Figure legends**
3

4 **Figure 1.** Idiopathic pulmonary fibrosis (IPF)/usual interstitial pneumonia (UIP) in a
5
6
7 50-year-old man (patient 13).

8
9 The high-resolution computed tomography image shows honeycombing (arrow) and
10
11 intralobular reticular opacity (arrowhead) in a predominantly peripheral distribution in the lower
12
13 lobe of the right lung.
14
15
16

17
18
19 **Figure 2.** Unclassified interstitial pneumonia in a 30-year-old man (patient 6).
20

21
22 A) The high-resolution computed tomography image shows diffuse reticulation and small air
23
24 cysts (arrows) in the peripheral zone in the middle and lower lobe of the right lung. The
25
26 diagnosis is “inconsistent with usual interstitial pneumonia (UIP) pattern.”
27

28
29 B) The pathologic specimen is stained with hematoxylin-eosin. The peripheral area of dense
30
31 fibrosis contains bronchiectatic spaces (arrows). The internal lung tissue is divided by fibrosis
32
33 connecting bronchioles or interlobular septa, which appears as “bridging fibrosis” (arrowheads).
34
35 Normal lung tissue remains in fibrous connection. The patient’s pathological diagnosis is “not
36
37
38
39
40
41
42
43
44
45
46
47
48
49
50
51
52
53
54
55
56
57
58
59
60
61
62
63
64
65
UIP”

66
67 **Figure 3.** Unclassified interstitial pneumonia in a 44-year-old woman (patient 8).
68

69
70 A) The high-resolution computed tomography image shows diffuse reticulation and traction
71
72 bronchiectasis (arrow) without macroscopic honeycombing in a random distribution in the
73
74 middle lobe of the right lung, and is diagnosed as “**indeterminate usual interstitial pneumonia**
75
76
77
78
79
80
81
82
83
84
85
86
87
88
89
90
91
92
93
94
95
96
97
98
99
100
101
102
103
104
105
106
107
108
109
110
111
112
113
114
115
116
117
118
119
120
121
122
123
124
125
126
127
128
129
130
131
132
133
134
135
136
137
138
139
140
141
142
143
144
145
146
147
148
149
150
151
152
153
154
155
156
157
158
159
160
161
162
163
164
165
166
167
168
169
170
171
172
173
174
175
176
177
178
179
180
181
182
183
184
185
186
187
188
189
190
191
192
193
194
195
196
197
198
199
200
201
202
203
204
205
206
207
208
209
210
211
212
213
214
215
216
217
218
219
220
221
222
223
224
225
226
227
228
229
230
231
232
233
234
235
236
237
238
239
240
241
242
243
244
245
246
247
248
249
250
251
252
253
254
255
256
257
258
259
260
261
262
263
264
265
266
267
268
269
270
271
272
273
274
275
276
277
278
279
280
281
282
283
284
285
286
287
288
289
290
291
292
293
294
295
296
297
298
299
300
301
302
303
304
305
306
307
308
309
310
311
312
313
314
315
316
317
318
319
320
321
322
323
324
325
326
327
328
329
330
331
332
333
334
335
336
337
338
339
340
341
342
343
344
345
346
347
348
349
350
351
352
353
354
355
356
357
358
359
360
361
362
363
364
365
366
367
368
369
370
371
372
373
374
375
376
377
378
379
380
381
382
383
384
385
386
387
388
389
390
391
392
393
394
395
396
397
398
399
400
401
402
403
404
405
406
407
408
409
410
411
412
413
414
415
416
417
418
419
420
421
422
423
424
425
426
427
428
429
430
431
432
433
434
435
436
437
438
439
440
441
442
443
444
445
446
447
448
449
450
451
452
453
454
455
456
457
458
459
460
461
462
463
464
465
466
467
468
469
470
471
472
473
474
475
476
477
478
479
480
481
482
483
484
485
486
487
488
489
490
491
492
493
494
495
496
497
498
499
500
501
502
503
504
505
506
507
508
509
510
511
512
513
514
515
516
517
518
519
520
521
522
523
524
525
526
527
528
529
530
531
532
533
534
535
536
537
538
539
540
541
542
543
544
545
546
547
548
549
550
551
552
553
554
555
556
557
558
559
560
561
562
563
564
565
566
567
568
569
570
571
572
573
574
575
576
577
578
579
580
581
582
583
584
585
586
587
588
589
590
591
592
593
594
595
596
597
598
599
600
601
602
603
604
605
606
607
608
609
610
611
612
613
614
615
616
617
618
619
620
621
622
623
624
625
626
627
628
629
630
631
632
633
634
635
636
637
638
639
640
641
642
643
644
645
646
647
648
649
650
651
652
653
654
655
656
657
658
659
660
661
662
663
664
665
666
667
668
669
670
671
672
673
674
675
676
677
678
679
680
681
682
683
684
685
686
687
688
689
690
691
692
693
694
695
696
697
698
699
700
701
702
703
704
705
706
707
708
709
710
711
712
713
714
715
716
717
718
719
720
721
722
723
724
725
726
727
728
729
730
731
732
733
734
735
736
737
738
739
740
741
742
743
744
745
746
747
748
749
750
751
752
753
754
755
756
757
758
759
760
761
762
763
764
765
766
767
768
769
770
771
772
773
774
775
776
777
778
779
780
781
782
783
784
785
786
787
788
789
790
791
792
793
794
795
796
797
798
799
800
801
802
803
804
805
806
807
808
809
810
811
812
813
814
815
816
817
818
819
820
821
822
823
824
825
826
827
828
829
830
831
832
833
834
835
836
837
838
839
840
841
842
843
844
845
846
847
848
849
850
851
852
853
854
855
856
857
858
859
860
861
862
863
864
865
866
867
868
869
870
871
872
873
874
875
876
877
878
879
880
881
882
883
884
885
886
887
888
889
890
891
892
893
894
895
896
897
898
899
900
901
902
903
904
905
906
907
908
909
910
911
912
913
914
915
916
917
918
919
920
921
922
923
924
925
926
927
928
929
930
931
932
933
934
935
936
937
938
939
940
941
942
943
944
945
946
947
948
949
950
951
952
953
954
955
956
957
958
959
960
961
962
963
964
965
966
967
968
969
970
971
972
973
974
975
976
977
978
979
980
981
982
983
984
985
986
987
988
989
990
991
992
993
994
995
996
997
998
999
1000

139 B) The pathologic image of the hematoxylin-eosin stained sample shows honeycombing

1 (arrows) in the peripheral zone (left side of the image) and inflammatory and fibrous changes
2
3
4 (arrowheads) without honeycombing in the internal zone (right side of the image), and is
5
6
7 diagnosed as “probable UIP (atypical).” The borders of the 2 zones are unclear. The size of
8
9
10 honeycombing is very small, as seen in idiopathic pulmonary fibrosis.
11
12
13
14
15
16
17
18
19
20
21
22
23
24
25
26
27
28
29
30
31
32
33
34
35
36
37
38
39
40
41
42
43
44
45
46
47
48
49
50
51
52
53
54
55
56
57
58
59
60
61
62
63
64
65

Table 1. Summary of Information on Patients, HRCT Diagnosis, Pathologic Diagnosis, and Multidisciplinary Diagnosis

Case No.	Age (y)/ Sex	CTD	Familial history of interstitial pneumonia	HRCT diagnosis (pattern)	Pathologic diagnosis	Multidisciplinary diagnosis
1	38/F	–	Yes	indeterminate UIP	UIP	possible IPF/UIP
2	46/M	rheumatoid arthritis	–	UIP	UIP	IP with CTD (UIP pattern)
3	29/F	unclassified CTD	–	inconsistent with UIP	probable UIP	IP with CTD (fibrotic NSIP pattern)
4	42/F	–	Yes	inconsistent with UIP	not UIP	unclassified IP
5	13/M	–	–	inconsistent with UIP	probable UIP	fibrotic NSIP
6	30/M	–	–	inconsistent with UIP	not UIP	unclassified IP
7	50/F	–	–	inconsistent with UIP	not UIP	unclassified IP
8	44/F	–	–	indeterminate UIP	probable UIP	unclassified IP
9	22/M	juvenile rheumatoid arthritis	–	inconsistent with UIP	UIP	IP with CTD (unclassified)
10	21/M	juvenile rheumatoid arthritis	Yes	inconsistent with UIP	probable UIP	IP with CTD (unclassified)
11	38/M	systemic sclerosis	Yes	inconsistent with UIP	UIP	IP with CTD (UIP pattern)
12	32/F	–	–	inconsistent with UIP	not UIP	unclassified IP
13	50/M	–	–	UIP	UIP	IPF/UIP
14	32/F	microscopic polyangiitis	Yes	inconsistent with UIP	not UIP	IP with CTD (unclassified)
15	35/M	Dermatomyositis	–	inconsistent with UIP	possible UIP	IP with CTD (fibrotic NSIP pattern)

HRCT = high-resolution computed tomography, CTD = connective tissue disease.

UIP = usual interstitial pneumonia, IPF = idiopathic pulmonary fibrosis, IP = interstitial pneumonia, NSIP = nonspecific interstitial pneumonia.

Table 2. HRCT Findings in All Patients

Findings	Number of patients (%)	Median extent (%)	Interquartile range of extent (%)
Intralobular reticular opacity	15 (100)	37.5	15–65
Air cysts	15 (100)	10	5–20
Ground glass opacity	15 (100)	5	5–10
Air space consolidation	13 (87)	5	5–10
Honeycombing	12 (80)	5	0–10
Traction bronchiectasis	15 (100)	–	–
Interlobular septal thickening	15 (100)	–	–
Distortion	12 (80)	–	–
Thickening of bronchovascular bundle	6 (40)	–	–
Centrilobular nodules	5 (33)	–	–

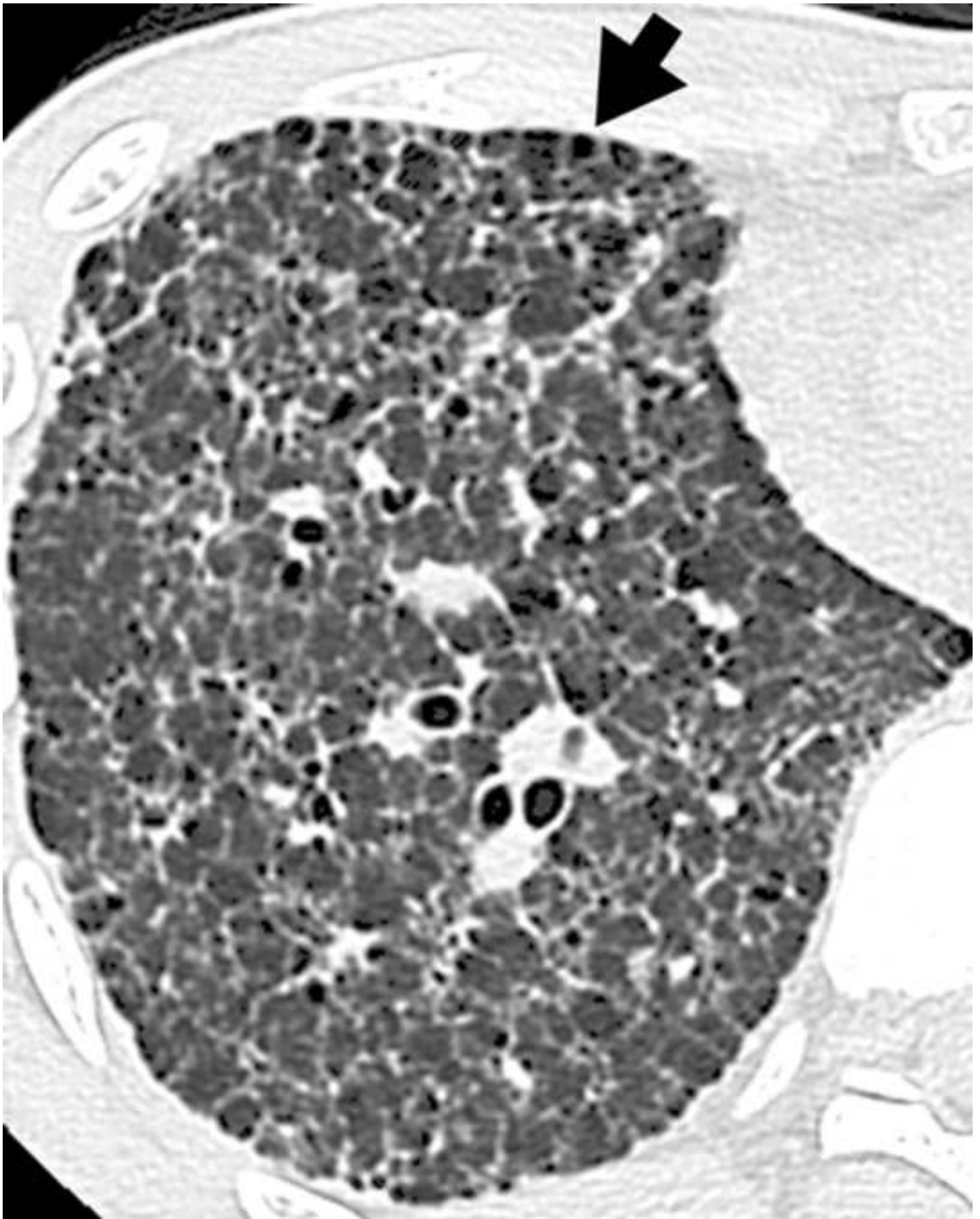
HRCT = high-resolution computed tomography

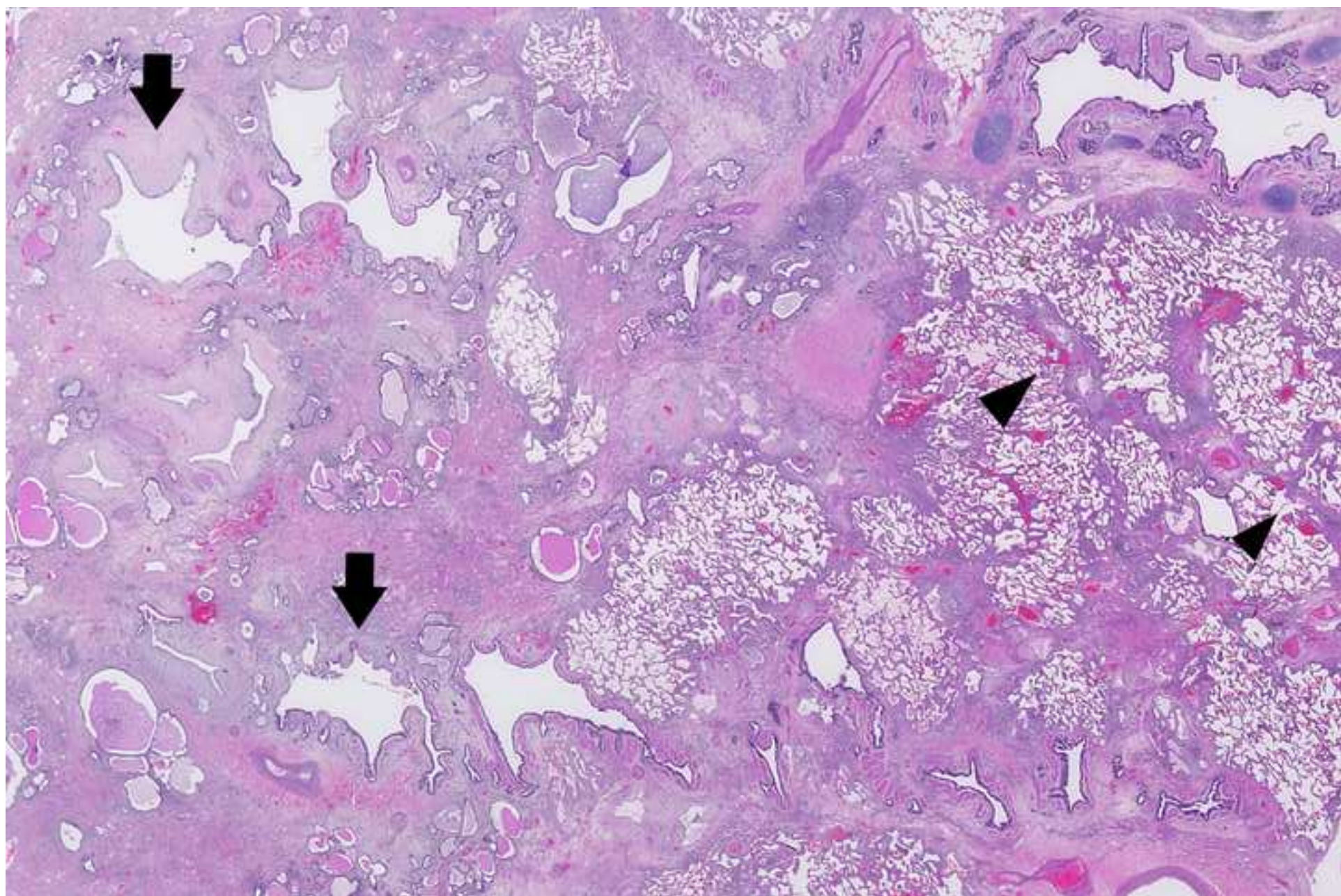
Table 3. Distribution of HRCT Abnormal Findings in Whole Lung

	Peripheral pattern	Peribronchovascular pattern	Diffuse pattern	Total (%)
Upper lung zone predominance	1	0	2	3 (20)
Lower lung zone predominance	1	5	0	6 (40)
Diffuse lung involvement	1	0	5	6 (40)
Total (%)	3 (20)	5 (33)	7 (47)	15 (100)

Figure 1







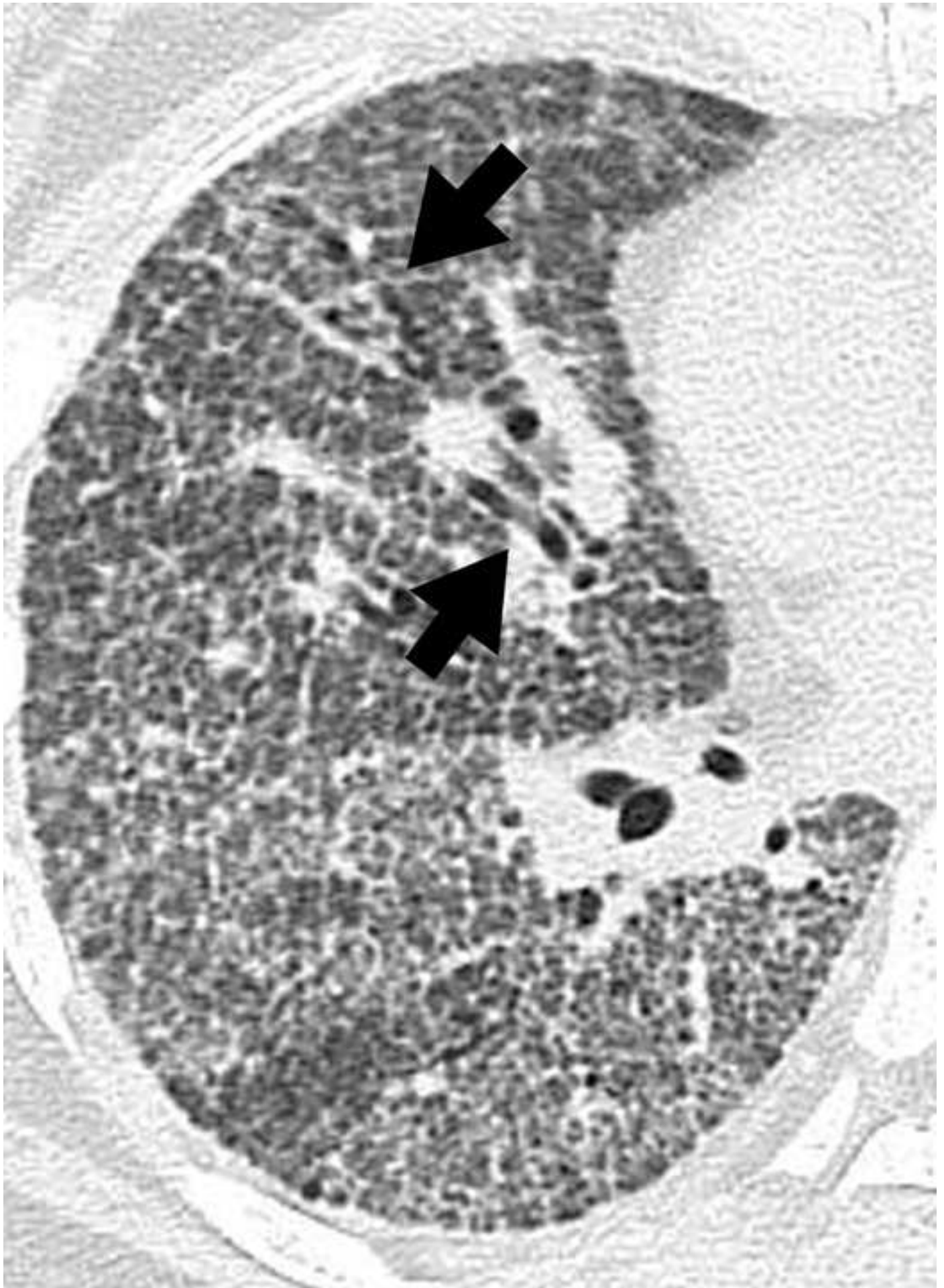


Figure 3B

